Journal of Applied Mechanics and Technical Physics, Vol. 43, No. 2, pp. 291–301, 2002

DYNAMIC PLASTIC DAMAGE OF SIMPLY AND DOUBLY CONNECTED ELLIPTIC PLATES

Yu. V. Nemirovsky and T. P. Romanova

UDC 539.3

This paper studies the dynamic behavior of simply and doubly connected elliptic ideal rigid-plastic plates with simply supported or clamped contours under short-time intensive dynamic loads. It is shown that there are several mechanisms of dynamic deformation of plates. For each mechanism, equations of the dynamic behavior are obtained. Operating conditions of these mechanisms are analyzed. Analytical expressions for the ultimate, "high" and "superhigh" loads and the maximum final deflection are obtained. Numerical examples are given.

Elliptic plates are frequently used as plugs and protective elements in mechanical engineering. Little information can be found in the literature on the analysis of these structures under high-intensity explosive loads [1]. In the present paper, a method of determining the final damage of simply and doubly connected elliptic plates subjected to short-time intensive dynamic loads is proposed. The final deflection of the plates serves as a measure of damage.

We consider a rigid-plastic plate with an elliptic contour l subjected to a uniformly distributed dynamic load of intensity $P(t)$. The plate contour can be simply supported or clamped.

Depending on the magnitude of the applied load, several mechanisms of dynamic deformation are possible. Under loads lower than the ultimate values ("low" loads), the plate remains at rest. For loads slightly higher than the ultimate values ("moderate" loads), as in the case of bending beams [2], circular and annular plates [3–8], and rectangular and polygonal plates [2, 9–12], a linear plastic hinge l_1 is formed and moves translationally in the plate (segment AB in Fig. 1 that shows mechanism No. 1). As a result, the plate is deformed into a certain ruled surface. For relatively high loads, the dynamics of the elliptic plate, as the dynamics of the structures mentioned above, can be accompanied by appearance, development, and disappearance of the region S_2 that moves translationally. For "high" loads, the region S_2 and a part of the hinge l_1 exist simultaneously (mechanism No. 2 shown in Fig. 2). For "superhigh" loads, the hinge l_1 vanishes (mechanism No. 3 shown in Fig. 3).

In all the aforementioned cases, any normal to the contour l intersects either the hinge l_1 or the curve l_2, i.e., the contour of the region S_2.

We write the equation of the ellipse l in a parametric form $x_1 = a\cos\varphi$ and $y_1 = b\sin\varphi$, where $0 \leqslant \varphi \leqslant 2\pi$ and $b \leqslant a$. The distance from the point $(x, y) \in Z$ to the hinge l_1 measured along the normal to l is denoted by $d_1(x, y)$, and the distance from the point $(x, y) \in S_1$ to the curve l_2 measured along l is denoted by $d_2(x, y)$ (Z is the part of the plate defined in such a manner that the normal to l passing through an arbitrary point of this part intersects l_1, and S_1 is the part of the plate defined in such a manner that the normal to l passing through an arbitrary point of this part intersects l_2) (see Figs. 1–3).

Since the plate is symmetric about the x and y axes and $b \leqslant a$, the hinge l_1 is a linear segment lying on the x axis: $-x_* \leqslant x \leqslant x_*$. We draw a normal to the contour l so that it intersects the x axis. Let us calculate the coordinates of the intersection point and determine their maximum value x_*.

The normal to the contour l at the point $[x_1(\varphi), y_1(\varphi)]$ is defined by the equation

$$-a\sin\varphi(x - a\cos\varphi) + b\cos\varphi(y - b\sin\varphi) = 0. \tag{1}$$

Institute of Theoretical and Applied Mechanics, Siberian Division, Russian Academy of Sciences, Novosibirsk 630090. Translated from Prikladnaya Mekhanika i Tekhnicheskaya Fizika, Vol. 43, No. 2, pp. 142–154, March–April, 2002. Original article submitted July 10, 2001.

0021-8944/02/4302-0291 $27.00

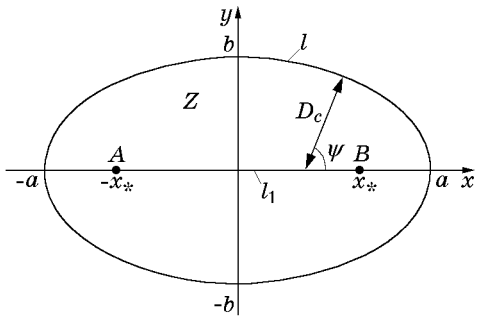

Fig. 1

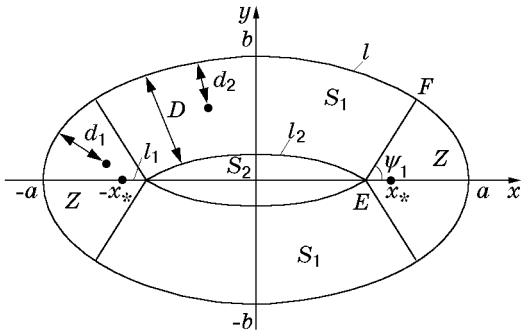

Fig. 2

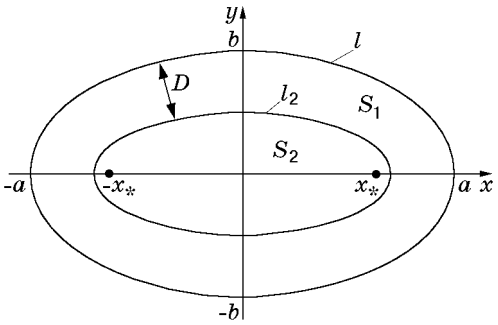

Fig. 3

The angle between the normal to the contour l and the x axis is

$$\psi = \arctan\left((a/b)\tan\varphi\right). \tag{2}$$

Here $x_l = (a - b^2/a)\cos\varphi$, where $(x_l, 0) \in l_1$ (x_l is the point of intersection of the normal and the x axis). Then, $x_* = \lim\limits_{\varphi\to 0} x_l = a - b^2/a$.

The distance D_c from the point $[x_1(\varphi), y_1(\varphi)]$ of the contour l to l_1 is

$$D_c = \sqrt{(x_1(\varphi) - x_l)^2 + y_1^2(\varphi)} = bL(\varphi)/a, \qquad L(\varphi) = \sqrt{a^2\sin^2\varphi + b^2\cos^2\varphi}. \tag{3}$$

The minimum and maximum distances from l to l_1 are determined by the formulas

$$D_{\min} = \min_{0\leqslant\varphi\leqslant\pi} D_c(\varphi) = b^2/a, \qquad D_{\max} = \max_{0\leqslant\varphi\leqslant\pi} D_c(\varphi) = b.$$

We show that a line normal to l is also normal to l_2. To this end, we approximate the contour l by a polygonal contour $\bar{l}$. For the polygonal plate obtained, the contour of the internal region, which moves translationally, becomes a polygonal contour $\bar{l}_2$. The authors [11] showed that the segments of the internal contour $\bar{l}_2$ are parallel to the corresponding segments of the contour $\bar{l}$. Hence, as the number of segments of the polygonal contour $\bar{l}$ tends to infinity, the contour $\bar{l}_2$ becomes closer and closer to l_2 and the normal to l at any point of this contour is also a normal to l_2.

To obtain the equation of the contour l_2, we draw the normal to l from the point $(x_1, y_1) \in l$ so that it intersects l_2. The distance between l and l_2 is written as $D = \delta R$ [$R(\varphi)$ is the radius of curvature of l and $\delta = \delta(\varphi, t) \geqslant 0$ is a dimensionless function]. The equation of l_2 has the form

$$x_2 = a\cos\varphi - \delta(a\cos\varphi - \xi), \qquad y_2 = b\sin\varphi - \delta(b\sin\varphi - \zeta).$$

Here $\xi = [1 - L^2(\varphi)/a^2]a\cos\varphi$ and $\zeta = [1 - L^2(\varphi)/b^2]b\sin\varphi$ are the coordinates of the center of curvature of the ellipse l at the point (x_1, y_1). Hence, we obtain

$$x_2 = [1 - \delta L^2(\varphi)/a^2]a\cos\varphi, \qquad y_2 = [1 - \delta L^2(\varphi)/b^2]b\sin\varphi. \tag{4}$$

The normal to l is also the normal to l_2. In this case, equality (1) holds for $x = x_2$ and $y = y_2$ and

$$x_2'(a\cos\varphi - x_2) + y_2'(b\sin\varphi - y_2) = 0, \qquad (\,\cdot\,)' = \partial(\,\cdot\,)/\partial\varphi.$$

This relation yields

$$x_2' b \cos\varphi + y_2' a \sin\varphi = 0. \tag{5}$$

Differentiating (4) and substituting the resulting relations into (5), we arrive at the equation for $\delta(\varphi, t)$

$$\delta' L^4(\varphi) + 3\delta L^2(\varphi)(a^2 - b^2)\sin\varphi\cos\varphi = 0.$$

Solving this equation, we obtain

$$\delta = \delta_0 ab/L^3, \qquad \delta_0 = \delta_0(t) \geqslant 0. \tag{6}$$

The radius of curvature of the ellipse l is $R(\varphi) = L^3/(ab)$. It follows from (6) that

$$D = \delta(\varphi, t)R(\varphi) = \delta_0(t). \tag{7}$$

Consequently, the distance D between the curves l and l_2 does not depend on the parameter φ. With allowance for (6) and (7), Eq. (4) for l_2 becomes

$$x_2 = [a - Db/L(\varphi)]\cos\varphi, \qquad y_2 = [b - Da/L(\varphi)]\sin\varphi.$$

The contour l_2 is not elliptic for $D > 0$. For the curve l_2 to have no mutually intersecting segments, the following conditions must be satisfied: $y_2 > 0$ for $0 < \varphi < \pi$ and $y_2 < 0$ for $\pi < \varphi < 2\pi$. Therefore, for the values of D in the interval $(b^2/a, b)$, the curve l_2 is determined not for all values of φ. The case $D > b$ corresponds to mechanism No. 1, where the region S_2 and the curve l_2 are absent, the case $b^2/a < D \leqslant b$ corresponds to mechanism No. 2, and the case $D \leqslant b^2/a$ corresponds to mechanism No. 3. In the case of a circular plate ($a = b$), mechanism No. 2 is skipped, and the hinge l_1 degenerates into a point, the plate center.

In the general case, the plate is deformed according to mechanism No. 2. In the absence of the regions S_2 and S_1, this mechanism becomes mechanism No. 1. If the region Z is absent, mechanism No. 2 becomes mechanism No. 3. Let us consider mechanism No. 2.

To obtain equations of motion of the plate, we use the virtual power principle and d'Alembert principle [13]:

$$K = A - N; \tag{8}$$

$$K = \iint\limits_S \rho \frac{\partial^2 u}{\partial t^2} \frac{\partial u^*}{\partial t}\, ds; \tag{9}$$

$$A = \iint\limits_S P(t) \frac{\partial u^*}{\partial t}\, ds; \tag{10}$$

$$N = \sum_m \int\limits_{l_m} M_m \Big[\frac{\partial \theta_m^*}{\partial t}\Big]\, dl. \tag{11}$$

Here K and A are the powers of inertial and external forces, respectively, S is the area of the plate, u is the deflection, ρ is the surface density of the plate material, N is the power of the internal forces of the plate, t is the current time, l_m are the lines of discontinuity in the angular velocities, M_m is the bending moment on l_m, and $[\partial\theta_m^*/\partial t]$ is the discontinuity in the angular velocity on l_m. In the expression for N, summation is performed for all lines of discontinuity in the angular velocity, including the plate boundary. The asterisk denotes the admissible velocities.

Since the velocities on the boundaries of the region S_2 and hinge l_1 are continuous and their motion is translational, the deflection rate in the region S_2 is equal to that on l_1. We denote it by $\dot{w}_c(t)$.

According to [14], we write the power of internal forces (11) as

$$N = M_0(2 - \eta) \oint\limits_l \frac{\partial \dot{u}^*}{\partial n}\, dl, \tag{12}$$

where M_0 is the limiting bending moment, $\eta = 0$ for the clamped contour, $\eta = 1$ for the simply supported contour, $\partial\dot{u}/\partial n$ is the derivative of the deflection rate with respect to the normal to the contour l or the angular velocity of rotation of the plate surface relative to the horizontal plane at the contour l, dl is the element of the contour l, and $\dot{(\cdot)} = \partial(\cdot)/\partial t$.

We denote the angle of rotation of the line EF [the boundary of the regions Z and S_1 (see Fig. 2)] about l by α. In the region S_1, the plate rotates about the supporting contour through the angle

$$\alpha_2(t) = \alpha(t). \tag{13}$$

In the region Z, this angle is equal to α_1. Since a part of the hinge l_1 moves at a constant translational velocity, we have

$$\alpha_1(t, \varphi) = \alpha D/D_c. \tag{14}$$

The position of the boundary EF is determined by the parameter $\varphi = \varphi_1$. It follows from (3) that the length of EF is

$$D = L(\varphi_1)b/a. \tag{15}$$

As a result, expression (12) for N becomes

$$N = M_0(2-\eta)\left[\int\limits_{\partial Z} \dot\alpha^* \frac{D}{D_c}\, dl + \int\limits_{\partial S_1} \dot\alpha^*\, dl\right].$$

The region Z is determined by the conditions $0 \leqslant \varphi \leqslant \varphi_1$, $\pi - \varphi_1 \leqslant \varphi \leqslant \pi + \varphi_1$, and $2\pi - \varphi_1 \leqslant \varphi \leqslant 2\pi$, and the region S_1 is determined by the conditions $\varphi_1 \leqslant \varphi \leqslant \pi - \varphi_1$ and $\pi + \varphi_1 \leqslant \varphi \leqslant 2\pi - \varphi_1$. In the region Z, the angle ψ varies within the intervals $0 \leqslant \psi \leqslant \psi_1$, $\pi - \psi_1 \leqslant \psi \leqslant \pi + \psi_1$, and $2\pi - \psi_1 \leqslant \psi \leqslant 2\pi$, where $\psi_1 = \psi(\varphi_1)$ and ψ is determined by (2). With allowance for (3), we obtain

$$\int\limits_{\partial Z} \dot\alpha^* \frac{D}{D_c}\, dl = 4\int\limits_0^{\varphi_1} (\dot\alpha^* D)\, \frac{\sqrt{x_1'^2 + y_1'^2}}{D_c}\, d\varphi = 4\dot\alpha^* D\varphi_1\, \frac{a}{b}, \qquad \int\limits_{\partial S_1} \dot\alpha^*\, dl = 4\dot\alpha^* \int\limits_{\varphi_1}^{\pi/2} L(\varphi)\, d\varphi.$$

Then, the expression for N takes the form

$$N = 4M_0(2-\eta)\dot\alpha^*\left[D\varphi_1\, \frac{a}{b} + \int\limits_{\varphi_1}^{\pi/2} L(\varphi)\, d\varphi\right]. \tag{16}$$

The deflection rate in the regions Z, S_1, and S_2 is given by

$$(x,y) \in Z\colon \quad \dot u = \dot\alpha_1 d_1, \qquad (x,y) \in S_1\colon \quad \dot u = \dot\alpha_2 d_2, \qquad (x,y) \in S_2\colon \quad \dot u = \dot w_c. \tag{17}$$

Expressions (9) and (10) become

$$K = \rho\left[\dot\alpha^*\ddot\alpha D^2 \iint\limits_Z \frac{d_1^2}{D_c^2}\, ds + \dot\alpha^*\ddot\alpha \iint\limits_{S_1} d_2^2\, ds + \dot w_c^*\ddot w_c \iint\limits_{S_2} ds\right]; \tag{18}$$

$$A = \dot\alpha^*\left[P(t)D \iint\limits_Z \frac{d_1}{D_1}\, ds + P(t) \iint\limits_{S_1} d_2\, ds\right] + \dot w_c^* P(t) \iint\limits_{S_2} ds. \tag{19}$$

To calculate the double integrals over the regions Z and S_1, we use the curvilinear orthogonal coordinate system (v_1, v_2) related to the Cartesian coordinate system by the relations

$$x = [a - v_1 b/L(v_2)]\cos v_2, \qquad y = [b - v_1 a/L(v_2)]\sin v_2.$$

The curves $v_1 = \text{const}$ are at the distance v_1 from the contour l. The lines $v_2 = \text{const}$ are normal to the elliptic contour.

Substituting (16), (18), and (19) into (8) and taking into account that $\dot\alpha^*$ and $\dot w_c^*$ are independent, we obtain the following equations of motion governing the deformation according to mechanism No. 2:

$$\rho\ddot\alpha D\Sigma_1 = P(t)\Sigma_2 - 12M_0(2-\eta)\Sigma_3; \tag{20}$$

$$\rho\ddot w_c = P(t). \tag{21}$$

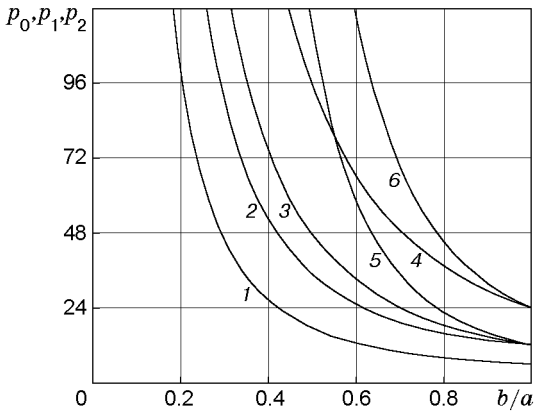

Fig. 4

Here

$$\Sigma_1 = (2a^2 - b^2)\varphi_1 - (a^2 - b^2)\sin 2\varphi_1 + D\,\frac{a}{b}\left[4\int\limits_{\varphi_1}^{\pi/2} L(\varphi)\,d\varphi - 3D\Big(\frac{\pi}{2} - \psi_1\Big)\right],$$

$$\Sigma_2 = (3a^2 - b^2)\varphi_1 - 1.5(a^2 - b^2)\sin 2\varphi_1 + 2D\,\frac{a}{b}\left[3\int\limits_{\varphi_1}^{\pi/2} L(\varphi)\,d\varphi - 2D\Big(\frac{\pi}{2} - \psi_1\Big)\right],$$

$$\Sigma_3 = \left[\varphi_1 + \frac{b}{aD}\int\limits_{\varphi_1}^{\pi/2} L(\varphi)\,d\varphi\right]\frac{a^2}{b^2}.$$

Since the rates are continuous on the boundaries of the regions S_1, S_2 and S_2, Z, then

$$\dot\alpha D = \dot w_c. \tag{22}$$

System (15), (20)–(22) describes the plate deformation according to mechanism No. 2. In the case of deformation according to mechanism No. 1, the regions S_1 and S_2 are absent, and the plate motion is described by Eqs. (20) and (22) for $\varphi_1 = \pi/2$ and $D = b$. If the plate is deformed according to mechanism No. 3, the region Z is absent, and the behavior of the plate is governed by Eqs. (20)–(22) for $\varphi_1 = 0$.

We consider the response of the plate to an impact load $P(t)$, which gradually increases from zero to a maximum value $P_{\max}$ and, then, decreases monotonically.

At the initial time, the plate is at rest:

$$\alpha(t_0) = \dot\alpha(t_0) = w_c(t_0) = \dot w_c(t_0) = 0. \tag{23}$$

If $0 < P_{\max} \leqslant P_0$ ("low" loads), where P_0 is the ultimate load, the plate remains at rest. We determine the quantity P_0 from Eq. (20) for $\ddot\alpha(t_0) = 0$, $\varphi_1 = \pi/2$, and $D = b$:

$$P_0 = 12M_0(2 - \eta)/[b^2(3 - b^2/a^2)].$$

For a circular plate of radius R, the ultimate load is $P_0 = 6M_0(2-\eta)/R^2$. In the simply supported case, this value is equal to the exact value of the ultimate load $\bar P_0$ obtained in [3]. For the clamped contour, the ultimate load calculated from the last formula is $2\bar P_0$ compared to the approximate value $1.875\bar P_0$ obtained in [5] using the Tresca yield criterion. Figure 4 shows the ultimate load p_0 versus the geometrical parameters of the ellipse ($p_0 = P_0a^2/M_0$). Curves 1 and 2 correspond to the simply supported and clamped contours, respectively.

The plate is deformed in accordance with mechanism No. 1 if $P_0 < P_{\max} \leqslant P_1$ ("moderate" loads), where P_1 is the load at which the regions S_1 and S_2 appear. To determine the load P_1, we differentiate (22) and use the resulting relation to eliminate $\ddot w_c$ and $\ddot\alpha$ from (20) and (21). As a result, we have

$$-\rho\dot\alpha\dot D\Sigma_1 = P(t)(\Sigma_2 - \Sigma_1) - 12M_0(2 - \eta)\Sigma_3. \tag{24}$$

At the moment the regions S_1 and S_2 appear, the region Z occupies the entire plate and $\varphi_1 = \pi/2$, $D = b$, and $\dot{D} = 0$. From (24), we obtain

$$P_1 = 12M_0(2-\eta)/b^2 > P_0. \tag{25}$$

For the circular plate, Eq. (25) yields $P_1 = 2P_0$. In the simply supported case, this result coincides with that obtained in [4, 6]. For the clamped contour, it was found that $P_1 = 1.998P_0$ (see [5]). Figure 4 shows the load p_1 versus the geometrical parameters of the ellipse ($p_1 = P_1a^2/M_0$). Curves 3 and 4 correspond to the simply supported and clamped contours, respectively.

For "moderate" loads, the plate motion is governed by Eqs. (20) and (22) for $\varphi_1 = \pi/2$ and $D = b$ with the initial conditions (23), where t_0 is determined under the condition $P(t_0) = P_0$. At the moment $t = T$, the load is removed and the plate moves inertially for some time. The time when the plate comes to rest t_f is determined from the condition

$$\dot{w}_c(t_f) = 0 \tag{26}$$

and it is given by the expression

$$t_f = t_0 + \frac{1}{P_0}\int\limits_{t_0}^{T} P(t)\,dt. \tag{27}$$

The deflections are calculated from (17) with allowance for (13) and (14). The final deflection at the plate center is

$$w_c(t_f) = \frac{3 - b^2/a^2}{\rho(2 - b^2/a^2)}\left[\frac{1}{2P_0}\left(\int\limits_{t_0}^{T} P(t)dt\right)^2 - \int\limits_{t_0}^{T}(t - t_0)P(t)\,dt\right].$$

For a simply supported circular plate, this result coincides with that obtained in [7].

If $P_1 < P_{\max} \leqslant P_2$ ("high" loads), where P_2 is the load for which the region Z vanishes, mechanism Nos. 1, 2, and 1 operate in succession.

The first phase ($t_0 < t \leqslant t_1$). The times t_0 and t_1 are determined from the conditions $P(t_0) = P_0$ and $P(t_1) = P_1$, respectively. The plate motion is described by Eqs. (20) and (22) for $\varphi_1 = \pi/2$ and $D = b$ with the initial conditions (23). At the time t_1, the regions S_1 and S_2 are formed. At this moment, the quantities $\alpha(t_1)$, $\dot{\alpha}(t_1)$, $w_c(t_1)$, and $\dot{w}_c(t_1)$ are determined.

The second phase ($t_1 < t \leqslant t_2$). At this stage of motion, the regions S_1 and S_2 develop. The region S_2 increases to a maximum size, then it decreases and vanishes at t_2. In the process, the region Z decreases but does not vanish. The plate motion is governed by Eqs. (15) and (20)–(22) subject to the initial conditions that correspond to the end of the first phase. In this case, $\varphi_1(t_1) = \pi/2$ and $D(t_1) = D_{\max} = b$.

At the time t_* when the region S_2 reaches the maximum size, the condition $\dot{D}(t_*) = 0$ holds. For the load considered, the region Z still exists and, hence, $D_{\min} \leqslant D(t_*)$. Taking into account that the region Z is absent and setting $P(t_*) = P_2$, $D(t_*) = D_{\min} = b^2/a$, and $\varphi_1 = 0$, we determine the load P_2 from (24). Using the approximate formula [15]

$$\int\limits_0^{\pi/2} L(\varphi)\,d\varphi \approx \frac{\pi Q}{8} \qquad [Q = 3(a+b) - 2\sqrt{ab}], \tag{28}$$

we obtain

$$P_2 = \frac{6M_0(2-\eta)}{(b^2/a)^2[1 - 2(b^2/a)/Q]}.$$

For the circular plate, we have $P_1 = P_2$, i.e., the "high" and "superhigh" loads coincide. Figure 4 shows the load p_2 versus the geometrical parameters of the ellipse ($p_2 = P_2a^2/M_0$). Curves 5 and 6 refer to the simply supported and clamped contours, respectively.

The second phase is completed at the time t_2 when $D(t_2) = D_{\max} = b$. At the end of the phase, the quantities $\alpha(t_2)$, $\dot{\alpha}(t_2)$, $w_c(t_2)$, and $\dot{w}_c(t_2)$ are determined.

The third phase ($t_2 < t \leqslant t_f$). The plate motion is described by Eqs. (20) and (22) for $\varphi_1 = \pi/2$, $D = b$, and the initial conditions that correspond to the end of the second phase. The moment the plate comes to rest is determined from (26). The deflections of the plate are calculated from (13), (14), and (17) with allowance for all phases of motion.

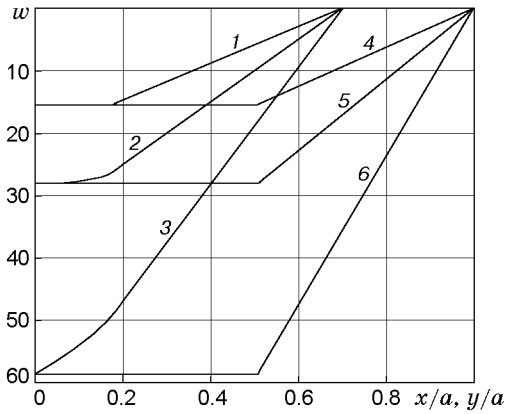

Fig. 5

If $P_{\max} > P_2$ ("superhigh" loads), mechanism Nos. 1–3 operate in succession. After reaching the maximum, the load decreases monotonically and mechanism Nos. 2 and 1 operate in succession.

The first phase ($t_0 < t \leqslant t_1$). This phase corresponds to the first phase of motion under "high" loads and is described by the same equations.

The second phase ($t_1 < t \leqslant t_2$). At this stage of motion, the regions S_1 and S_2 develop according to mechanism No. 2, and the region Z decreases and vanishes at the time t_2 determined from the relation $P(t_2) = P_2$. The plate motion is described by Eqs. (15), and (20)–(22) subject to the initial conditions determined at the end of the first phase. At the end of the second phase, the quantities $\alpha(t_2)$, $\dot\alpha(t_2)$, $w_c(t_2)$, and $\dot w_c(t_2)$ are calculated.

The third phase ($t_2 < t \leqslant t_3$). At this stage of motion, the plate is deformed in accordance with mechanism No. 3. The behavior of the plate is described by Eqs. (20)–(22) for $\varphi_1 = 0$ subject to the initial conditions determined at the end of the second phase. At a certain time t_{**}, the region S_2 reaches the maximum size. In this case, we have $D(t_{**}) = D_{**}$ and $\dot D(t_{**}) = 0$. Setting $\varphi_1 = 0$ in (24) and using (28), we obtain

$$P(t_{**})D_{**}^2(1 - 2D_{**}/Q) = 6M_0(2 - \eta).$$

The time t_3 (when the region Z is formed) is determined from the condition $D(t_3) = D_{\min} = b^2/a$. At the end of the third phase, the quantities $\alpha(t_3)$, $\dot\alpha(t_3)$, $w_c(t_3)$, and $\dot w_c(t_3)$ are calculated.

The fourth phase ($t_3 < t \leqslant t_4$). At this stage of motion, the region S_2 continues to decrease according to mechanism No. 2. At the time t_4, the region S_2 vanishes and the region Z occupies the entire plate. The plate motion is described by Eqs. (15) and (20)–(22) subject to the initial conditions determined at the end of the third phase. The time t_4 is determined from the condition $D(t_4) = D_{\max} = b$. At the end of the fourth phase, the quantities $\alpha(t_4)$, $\dot\alpha(t_4)$, $w_c(t_4)$, and $\dot w_c(t_4)$ are determined.

The fifth phase ($t_4 < t \leqslant t_f$). At this stage, the plate is deformed according to mechanism No. 1 until it comes to complete rest at the time t_f determined from (26). The plate motion is described by Eqs. (20) and (22) for $\varphi_1 = \pi/2$ and $D = b$.

The deflections are determined by (13), (14), and (17) with allowance for all phases of motion. Figure 5 shows the curves $w(x/a)$ and $w(y/a)$ [$w = ua^2\rho/(M_0T^2)$] for the simply supported elliptic plate with the semiaxes ratio $b/a = 0.7$, subjected to a "high" load represented by a rectangular pulse: $P = 31.5M_0/a^2$ for $0 \leqslant t \leqslant T$ and $P = 0$ for $t > T$. Curves 1–3 refer to the deflections in the cross section $x = 0$ at the times $t = T$, $t = t_p = 1.39T$, and $t = t_f = 3.34T$, respectively (t_p is the moment the region S_2 vanishes). Curves 4–6 refer to the deflections in the cross section $y = 0$ at the same moments.

Let us consider a plate with an elliptic contour l and a supported internal hole determined by the parametric equations

$$x = [a - \lambda b/L(\varphi)]\cos\varphi, \qquad y = [b - \lambda a/L(\varphi)]\sin\varphi,$$

where λ is the distance from the external contour to the hole in the plate ($0 < \lambda \leqslant b^2/a$ and $\lambda = \text{const}$) (Fig. 6). In this case, the equations of the boundaries L_i ($i = 1, 2$) of the region S_2, which moves translationally, are similar to the equation of the curve l_2 of the plate without a hole:

$$x_{li} = [a - D_i b/L(\varphi)]\cos\varphi, \qquad y_{li} = [b - D_i a/L(\varphi)]\sin\varphi.$$

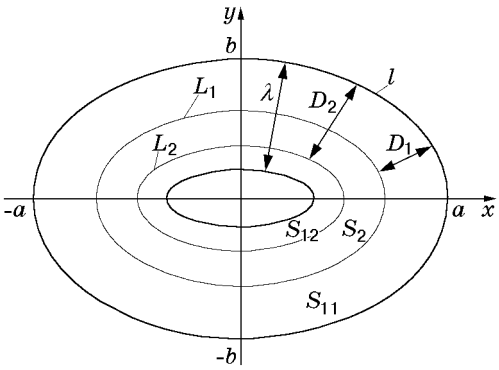

Fig. 6

Here D_i is the distance from the contour l to the boundary L_i and $0 < D_1 \leqslant D_2 < \lambda$ (Fig. 6).

For the chosen shape of the internal contour, the region S_2, which moves translationally, arrives simultaneously at all points of the curve l_1 where the following equality holds:

$$D_1 = D_2. \tag{29}$$

We denote the parts of the plate adjacent to the internal and external contours by S_{11} and S_{12}, respectively. Let β_i $(i = 1,\ 2)$ be the angle of rotation of the region S_{1i} about the supported contour. As in the case of the simply connected plate, the system of equations of motion of the doubly connected plate considered comprises Eq. (21) and

$$\rho\ddot{\beta}_1 D_1\Sigma_{11} = P(t)\Sigma_{12} - 12M_0(2-\eta_1)\Sigma_{13}; \tag{30}$$

$$\rho\ddot{\beta}_2(\lambda - D_2)\Sigma_{21} = P(t)\Sigma_{22} - 12M_0(2-\eta_2)\Sigma_{23}; \tag{31}$$

$$\dot{\beta}_1 D_1 = \dot{w}_c; \tag{32}$$

$$\dot{\beta}_2(\lambda - D_2) = \dot{w}_c, \tag{33}$$

where $\eta_i = 0$ for the clamped contour and $\eta_i = 1$ for the simply supported contour (the subscripts $i = 1$ and 2 refer to the external and internal contours, respectively),

$$\Sigma_{11}(D_1) = 4\int\limits_0^{\pi/2} L(\varphi)\,d\varphi - 3D_1\,\frac{\pi}{2}, \qquad \Sigma_{12}(D_1) = 2\left(3\int\limits_0^{\pi/2} L(\varphi)\,d\varphi - D_1\pi\right),$$

$$\Sigma_{13}(D_1) = D_1^{-2}\int\limits_0^{\pi/2} L(\varphi)\,d\varphi, \qquad \Sigma_{21}(D_2) = 4\int\limits_0^{\pi/2} L(\varphi)\,d\varphi - (\lambda + 3D_2)\frac{\pi}{2},$$

$$\Sigma_{22}(D_2) = 2\left(3\int\limits_0^{\pi/2} L(\varphi)\,d\varphi - \frac{(\lambda+2D_1)\pi}{2}\right), \qquad \Sigma_{23}(D_2) = \frac{1}{(\lambda - D_2)^2}\left(\int\limits_0^{\pi/2} L(\varphi)\,d\varphi - \frac{\lambda\pi}{2}\right).$$

In the case where the region S_2 degenerates into a curve, relation (29) is satisfied. The initial conditions have the form

$$\beta_i(t_0) = \dot{\beta}_i(t_0) = w_c(t_0) = \dot{w}_c(t_0) = 0, \qquad D_i(t_0) = D_{i0} \quad (i = 1, 2). \tag{34}$$

The values of D_{i0} are determined below.

The ultimate load P_0^* is determined from (30) and (31) by setting $\ddot{\beta}_i = 0$ $(i = 1, 2)$ and taking into account (28). As a result, we have

$$P_0^* = \frac{6M_0(2-\eta_1)}{D_0^2(3 - 8D_0/Q)},$$

where D_0 is found from the relation

$$\frac{2-\eta_1}{D_0^2(3-8D_0/Q)} = \frac{(2-\eta_2)(1-4\lambda/Q)}{(\lambda - D_0)^2[3 - 4(\lambda + 2D_0)/Q]}.$$

Let the plate be loaded by a rectangular pulse: $P = \text{const}$ for $0 \leqslant t \leqslant T$ and $P = 0$ for $t > T$. In this case, the functions $D_i(t)$ $(i = 1, 2)$ remain constant during loading. For $0 < P \leqslant P_0^*$ ("low" loads), the plate is not deformed and remains at rest. For $P_0^* < P \leqslant P_1^*$ ("moderate" loads), the region S_2 is absent. We determine the load P_1^*, for which the region S_2 is formed. Differentiating (32) and (33) with respect to time with allowance for (21) and substituting the resulting expressions into (30) and (31), we obtain

$$P\Sigma_{11} = P\Sigma_{12} - 12M_0(2-\eta_1)\Sigma_{13}; \tag{35}$$

$$P\Sigma_{21} = P\Sigma_{22} - 12M_0(2-\eta_2)\Sigma_{23}. \tag{36}$$

At the moment the region S_2 is formed, relation (29) holds. Hence, Eqs. (28), (35), and (36) yield

$$P_0^* = \frac{6M_0(2-\eta_1)}{D_p^2(1-2D_p/Q)},$$

where D_p is the value of D_1 for $P = P_1^*$, which is determined from the relation

$$\frac{2-\eta_1}{D_p^2(1-2D_p/Q)} = \frac{(2-\eta_2)(1-4\lambda/Q)}{(\lambda-D_p)^2[1-2(\lambda+D_p)/Q]}.$$

For the "moderate" load, the motion of the doubly connected elliptic plate for $0 \leqslant t \leqslant T$ (first phase) is described by Eqs. (29)–(33) subject to the initial conditions (34), where the quantity D_{10} is determined as follows. Differentiating (32) and (33) with respect to time, eliminating $\ddot{w}_c$, and substituting relations (28)–(31) into the resulting expression, we obtain the following equation forD_{10}:

$$P\lambda\Big(1-\frac{4D_{10}}{Q}\Big) = 6M_0\Big[\frac{2-\eta_1}{D_{10}^2}\Big(1-\frac{\lambda+3D_{10}}{Q}\Big) - \frac{2-\eta_2}{(\lambda-D_{10})^2}\Big(1-\frac{4\lambda}{Q}\Big)\Big(1-\frac{3D_{10}}{Q}\Big)\Big].$$

From the equations of motion, we find that

$$\dot\beta_1(t) = \frac{tF}{\rho D_{10}}, \quad \dot\beta_2(t) = \frac{tF}{\rho(\lambda-D_{10})}, \quad \dot w_c(t) = \frac{tF}{\rho}, \quad \beta_1(t) = \frac{t^2F}{2\rho D_{10}},$$

$$\beta_2(t) = \frac{t^2F}{2\rho(\lambda-D_{10})}, \quad w_c(t) = \frac{t^2F}{2\rho}, \quad F = \frac{\Sigma_{12}(D_{10})}{\Sigma_{11}(D_{10})}(P-P_0^*).$$

At the end of the first phase $(t = T)$, we have

$$\begin{gathered}\dot\beta_1(T) = \frac{TF}{\rho D_{10}}, \quad \dot\beta_2(T) = \frac{TF}{\rho(\lambda-D_{10})}, \quad \dot w_c(T) = \frac{TF}{\rho},\\ \beta_1(T) = \frac{T^2F}{2\rho D_{10}}, \quad \beta_2(T) = \frac{T^2F}{2\rho(\lambda-D_{10})}, \quad w_c(T) = \frac{T^2F}{2\rho}.\end{gathered} \tag{37}$$

In the second phase $(T < t \leqslant t_f)$, the behavior of the plate is described by a system that comprises Eqs. (29), (32), (33), and

$$\rho\ddot\beta_1 D_1\Sigma_{11} = -12M_0(2-\eta_1)\Sigma_{13}; \tag{38}$$

$$\rho\ddot\beta_2(\lambda-D_1)\Sigma_{21} = -12M_0(2-\eta_2)\Sigma_{23} \tag{39}$$

subject to the initial conditions (37) and $D_1(T) = D_{10}$. Differentiating (32) and (33) with respect to time and eliminating $\ddot{w}_c$, we obtain

$$\ddot\beta_2(\lambda-D_1) = \ddot\beta_1 D_1 + \dot\beta_1\dot D_1\lambda/(\lambda-D_1).$$

This relation can be combined with (38) and (39) to give

$$\dot D_1\,\frac{\dot\beta_1\lambda}{\lambda-D_1} = \frac{12M_0}{\rho}\Big(\frac{(2-\eta_1)\Sigma_{13}}{\Sigma_{11}} - \frac{(2-\eta_2)\Sigma_{23}}{\Sigma_{21}}\Big). \tag{40}$$

System (38)–(40) is solved by a numerical method. The moment at which the plate comes to rest is determined from condition (26). It follows from (26), (32), and (38) that the quantity $D_1(t_f) = D_f$ satisfies the equation

$$(2-\eta_1)\Sigma_{13}(D_f)/\Sigma_{11}(D_f) = (2-\eta_2)\Sigma_{23}(D_f)/\Sigma_{21}(D_f).$$

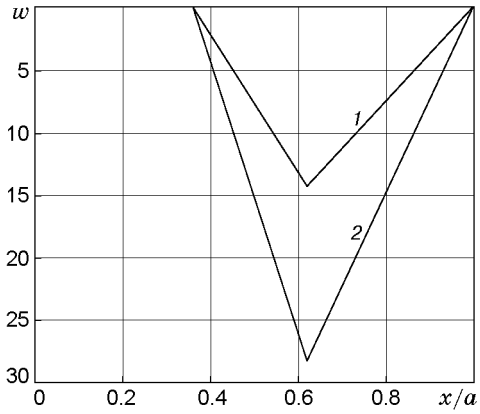

Fig. 7

The deflections of the doubly connected elliptic plate are determined from the equations

$$(x,y) \in S_{11}\colon\ \dot u = \dot\beta_1(t)d(x,y), \quad (x,y) \in S_{12}\colon\ \dot u = \dot\beta_2(t)d(x,y), \quad (x,y) \in S_2\colon\ \dot u = \dot w_c, \tag{41}$$

where $d(x,y)$ is the distance from the point (x,y) to the supporting part of the plate where this point is located.

A numerical analysis shows that the quantities D_0, D_p, D_{10} (for $P_0^* \leqslant P \leqslant P_1^*$), and D_f differ only slightly. Therefore, one can use an approximate analytical method based on the assumption that $D_1 = \text{const}$ to solve the problem. In this case, system (29)–(33) is replaced by system (29), (30), (32), (33) with $D_1 = \text{const}$, whose solution has the form

$$w_c(T) = \frac{3 - 8D_1/Q}{4\rho(1 - 3D_1/Q)}\,T^2(P - P_0^*), \quad w_c(t_f) = \frac{3 - 8D_1/Q}{4\rho(1 - 3D_1/Q)}\,T^2\frac{P^2}{P_0^*}\Big(1 - \frac{P_0^*}{P}\Big), \quad t_f = \frac{PT}{P_0^*}.$$

The maximum final deflection obtained by solving system (29)–(33) by the Runge–Kutta method differs from that determined by solving analytically system (29), (30), (32), (33) for $D_1 = (D_0 + D_p)/2$ by no more than 2%. Figure 7 shows the curves $w(x/a)$ calculated by the analytical method for a doubly connected elliptic plate loaded by a "moderate" rectangular pulse: $P = 37M_0/a^2$. The plate is characterized by the semiaxes ratio $b/a = 0.8$ and $\lambda = b^2/a$, and its both contours are simply supported. Curve 1 refers to the deflection at the time $t = T$ and curve 2 to the moment the plate ceases to move $t = t_f = 1.97T$.

The approximate system (29), (30), (32), (33) for $D_1 = \text{const}$ can be solved in the case of "moderate" loading by a pulse of an arbitrary form: $P(t_0) = P_0^*$; $P(t) \leqslant P_1^*$ for $t_0 \leqslant t \leqslant T$ and $P(t) = 0$ for $t > T$. It follows from the solution of this system that the time t_f at which the plate comes to rest is determined from (27), and the maximum final deflection is

$$w_c(t_f) = \frac{3 - 8D_1/Q}{4\rho(1 - 3D_1/Q)}\left[\frac{1}{P_0}\left(\int_{t_0}^{T} P(t)\,dt\right)^2 - 2\int_{t_0}^{T}(t - t_0)P(t)\,dt\right].$$

For a "high" load ($P > P_1^*$), the first phase of motion of the doubly connected elliptic plate ($0 \leqslant t \leqslant T$) is described by Eqs. (21) and (30)–(33) subject to the initial conditions (34). The values of D_{i0} ($i = 1, 2$) are determined from Eqs. (35) and (36). At the end of the first phase, we have

$$\begin{gathered}\dot\beta_1(T) = \frac{PT}{\rho D_{10}}, \quad \dot\beta_2(T) = \frac{PT}{\rho(\lambda - D_{20})}, \quad \dot w_c(T) = \frac{PT}{\rho}, \\ \beta_1(T) = \frac{PT^2}{2\rho D_{10}}, \quad \beta_2(T) = \frac{PT^2}{2\rho(\lambda - D_{20})}, \quad w_c(T) = \frac{PT^2}{2\rho}.\end{gathered} \tag{42}$$

In the second phase ($T < t \leqslant t_1$), the region S_2 is compressed and the plate motion is described by the system of equations (32), (33), (38), (39), and

$$\ddot w_c = 0 \tag{43}$$

subject to the initial conditions (42). It follows from (43) that

$$\dot w_c(t) = \dot w_c(T) = PT/\rho, \tag{44}$$

whence $w_c(t) = PTt/\rho$. Differentiating (32) and (33) with respect to t, taking into account (43), and inserting the resulting relations into (38) and (39) [with allowance for (32), (33), and (44)], we obtain

$$\dot{D}_1 = 12M_0(2-\eta_1)\Sigma_{13}D_1/(\Sigma_{11}PT), \qquad \dot{D}_2 = -12M_0(2-\eta_2)\Sigma_{23}(\lambda - D_2)/(\Sigma_{21}PT). \tag{45}$$

System (38), (39), (45) is solved by a numerical method. The time t_1 at which the region S_2 vanishes is determined from (29). At the end of the second phase, the quantities $\dot{\beta}_i(t_1)$, $\beta_i(t_1)$ $(i = 1, 2)$, $\dot{w}_c(t_1) = PT/\rho$, and $w_c(t_1) = PTt_1/\rho$ are determined.

In the third phase ($t_1 < t \leqslant t_f$), the motion is similar to the motion in the second phase for a "moderate" load.

The deflections of the plate are determined from (41) with allowance for all phases of motion.

REFERENCES

1. V. N. Mazalov and Yu. V. Nemirovsky, "Dynamics of thin-walled plastic structures," in: *Dynamic Problems of Plastic Media*, *Ser. Mech.* (collected scientific papers) [in Russian], No. 5 (1975), pp. 155–247.
2. K. L. Komarov and Yu. V. Nemirovsky, *Dynamics of Rigid-Plastic Structural Elements* [in Russian], Nauka, Novosibirsk (1984).
3. H. G. Hopkins and W. Prager, "The load-carrying capacities of circular plates," *J. Mech. Phys. Solids*, **2**, No. 1, 1–13 (1953).
4. H. G. Hopkins and W. Prager, "On the dynamics of plastic circular plates," *Z. Angew. Math. Phys.*, **5**, No. 4, 317–330 (1954).
5. A. L. Florence, "Clamped circular rigid-plastic plates under blast loading," *Trans. ASME, Ser. E, J. Appl. Mech.*, **33**, No. 2 (1966).
6. P. Perzyna, "Dynamic load carrying capacity of circular plate," *Arch. Mech. Stos.*, **10**, No. 5, 635–647 (1958).
7. C. K. Youngdahl, "Influence of pulse on the final plastic deformation of a circular plate," *Int. J. Solids Struct.*, **7**, No. 9, 1127–1142 (1971).
8. A. L. Florence, "Annular plate under a transverse line pulse," *AIAA J.*, **3**, No. 9, 1726–1733 (1965).
9. E. Virma, "Dynamics of plastic rectangular plates," *Uch. Zap. Tart. Univ.*, No. 305, 289–299 (1972).
10. N. Jones, T. O. Uran, and S. A. Tekin, "The dynamic plastic behaviour of fully clamped rectangular plates," *Int. J. Solids Struct.*, **6**, No. 2, 1499–1512 (1970).
11. Yu. V. Nemirovsky and T. P. Romanova, "Dynamic bending of polygonal plastic slabs," *J. Appl. Mech. Tech. Phys.*, **29**, No. 4, 591–597 (1988).
12. Yu. V. Nemirovsky and T. P. Romanova, "Dynamic behavior of doubly connected polygonal plastic plates," *Prikl. Mekh.*, **23**, No. 5, 52–59 (1987).
13. M. I. Erkhov, *Theory of Ideal Plastic Solids and Structures* [in Russian], Nauka, Moscow (1978).
14. A. R. Rzhanitsyn, *Structural Mechanics* [in Russian], Vysshaya Shkola, Moscow (1982).
15. I. N. Bronshtein and K. A. Semendyaev, *Mathematical Handbook* [in Russian], Nauka, Moscow (1986).